

# SUSY Phases, the Electron Electric Dipole Moment and the Muon Magnetic Moment

R. Arnowitt, B. Dutta and Y. Santoso

*Center For Theoretical Physics, Department of Physics,  
Texas A&M University, College Station TX 77843-4242*

(June, 2001)

## Abstract

The electron electric dipole moment ( $d_e$ ) and the muon magnetic moment anomaly ( $a_\mu$ ) recently observed at BNL are analyzed within the framework of SUGRA models with CP violating phases at the GUT scale. It is seen analytically that even if  $d_e$  were zero, there can be a large Bino mass phase (ranging from 0 to  $2\pi$ ) with a corresponding large  $B$  soft breaking mass phase (of size  $\lesssim 0.5$  with sign fixed by the experimental sign of  $a_\mu$ ). The dependence of the  $B$  phase on the other SUSY parameters, gaugino mass  $m_{1/2}$ ,  $\tan\beta$ ,  $A_0$ , is examined. The lower bound of  $a_\mu$  determines the upper bound of  $m_{1/2}$ . It is shown analytically how the existence of a non-zero Bino phase reduces this upper bound (which would correspondingly lower the SUSY mass spectra). The experimental upper bound on  $d_e$  determines the range of allowed phases, and the question of whether the current bound on  $d_e$  requires any fine tuning is investigated. At the electroweak scale, the phases have to be specified to within a few percent. At the GUT scale, however, the  $B$  phase requires fine tuning below the 1% level over parts of the parameter space for low  $m_{1/2}$ , and if the current experimental bound on  $d_e$  were reduced by only a factor of 3–4, fine tuning below 1% would occur at both the electroweak and GUT scale over large regions of the parameter space. All accelerator constraints ( $m_h > 114$  GeV,  $b \rightarrow s\gamma$ , etc.) and relic density constraints with all stau-neutralino co-annihilation processes are included in the analysis.

## I. INTRODUCTION

The role that CP violation plays in elementary particle physics and how it relates to current theory, still remains after many years unclear. In the Standard Model (SM), CP violation is accommodated by inserting a single phase into the CKM matrix, and there are now under way a number of experiments to test the validity of this idea [1]. In supersymmetry, the CKM phase can also exist, but it is possible to have additional phases appearing in the soft breaking masses. From the viewpoint of string theory, CP violating phases are a natural occurrence. Thus in 10 or 11 dimensional M-theory models with six dimensions compactified on a Calabi-Yau manifold, the Kahler potential and Yukawa matrices are represented by integrals over the Calabi-Yau space, and since this is a complex manifold, it is not surprising that CP violating phases can arise. With supersymmetry breaking, phases could arise also in the soft breaking masses. However, M-theory is not sufficiently developed to determine the details of such effects, and it is useful to have phenomenological constraints as a guide to where the fundamental theory may be.

As is well known, the existence of CP violating phases in the SUSY soft breaking masses leads to electric dipole moments (EDMs) for the electron and neutron, and the smallness of the current experimental bounds on these puts severe constraints on the parameter space. One may satisfy these constraints by assuming that the phases are non-zero but small (i.e.  $O(10^{-2})$ ) or that the SUSY masses are large (i.e.  $\gtrsim O(1 \text{ TeV})$ ). The electron EDM (eEDM) arises from two diagrams, one involving the chargino-sneutrino intermediate state, and one involving the neutralino-selectron intermediate state. More recently it was suggested that a cancellation might occur between these two for relatively large phases (i.e.  $O(10^{-1})$ ) over a reasonably large range of parameters [2], and there has been a large number of analyses based on this idea [3–6]. Diagrams similar to the above also enter into the muon  $g - 2$ , and the recently reported 2.6  $\sigma$  deviation from the Standard Model value for that quantity [7] has placed significant bounds (at the 95% C.L.) on the allowed SUGRA parameter space [8]. It is thus natural to ask whether both constraints can be phenomenologically realized, and initial discussions of this have been made [9].

The minimal supersymmetric standard model (MSSM) has over 40 independent phases, and so cannot make significant theoretical predictions on this question. We use here instead supergravity (SUGRA) GUT models with gravity mediated supersymmetry breaking [10] and R-parity invariance<sup>1</sup>. Such models have become quite predictive, in part due to the fact that they automatically include the LEP results on grand unification, and because radiative breaking of  $SU(2) \times U(1)$  implies that the SUSY soft breaking masses are of electroweak size. Thus the general size of both  $g - 2$  and the EDMs (which depend on the size of the SUSY masses) are restricted. In addition, such models have a natural candidate for dark matter, the lightest neutralino ( $\tilde{\chi}_1^0$ ), and the condition that the relic density of neutralinos be in accord with the allowed range from astronomical measurements also puts important

---

<sup>1</sup>Two alternate SUGRA models are anomaly mediated [11] and gauge mediated [12] soft breaking. The former appears to have difficulty in satisfying the Brookhaven E821 bounds on  $g - 2$  when no SUSY CP phases are present [13], while the latter does not appear to have a satisfactory dark matter candidate [14].

constraints on the parameter space.

Previous analyses of the EDMs within the framework of SUGRA GUT models has shown that a new fine tuning problem arises at the GUT scale for  $\theta_{B_0}$  (the phase of  $B$ , the bilinear soft breaking mass) when  $\tan\beta$  gets large [4]. Further, the discussion of the muon  $g-2$  have shown that  $\tan\beta$  is greater than 5 ( and very possibly greater than 10). In carrying out our analysis, then, we put a constraint on the parameter space that  $\Delta\theta_{B_0}/\theta_{B_0} > 0.01$ , where  $\Delta\theta_{B_0}$  is the allowed range that will satisfy the experimental bounds on the EDMs. In order to carry out a complete analysis, however, it is necessary to include all the accelerator constraints (i. e. that  $m_h > 114$  GeV (where  $h$  is the light Higgs boson), the CLEO bound on the  $b \rightarrow s\gamma$  decay, etc.) as well as the full analysis of the relic density including all the stau-neutralino co-annihilation channels. (The details of these were discussed in [15,16].)

Both the electron EDM and the muon  $g-2$  can be calculated from two types of diagrams, one with the intermediate chargino and sneutrinos states, and one with the intermediate neutralino and slepton states. If one assumes universal soft breaking in the first two generations, then the eEDM and the SUSY deviation of the muon magnetic moment from its Standard Model value,  $a_\mu^{\text{SUSY}}$  ( $a_\mu = (g_\mu - 2)/2$ ), can both be calculated from a single amplitude for these diagrams, the former being related to the imaginary part, and the latter to the real part. In the following we will use the symbol  $a_\mu$  to mean the deviation of the muon  $(g_\mu - 2)/2$  from its Standard Model value.

As is well known, for large  $\tan\beta$ ,  $a_\mu$  is dominated by the chargino diagram [17,18] (the neutralino diagrams being generally quite small), while the strong experimental constraints on the eEDM require a near cancellation between the neutralino and chargino diagrams [2]. In order to see how this can come about when CP violating phases are present, we calculate in the Appendix the leading large  $\tan\beta$  terms. We discuss analytically in Sec. 2 how both experimental constraints can naturally be satisfied at the electroweak scale. In Sec. 3 we examine in detail numerically the combined experimental constraints of the eEDM and the Brookhaven E821  $a_\mu$  experiment on the SUSY parameter space for a variant of the mSUGRA model where the magnitudes of the soft breaking masses are universal at  $M_G$  but the phases are arbitrary. The experimental lower bound on  $a_\mu$  puts an upper bound on the gaugino mass  $m_{1/2}$ , and this upper bound is generally reduced when CP violating phases are present. The Higgs mass lower bound and the  $b \rightarrow s\gamma$  constraint generally put a lower bound on  $m_{1/2}$ . Imposing the fine tuning constraint at  $M_{\text{GUT}}$  generally increases that bound when CP violating phases are present and also limits the range of the CP violating phases. Thus the two experiments interact to further restrict the SUSY parameter space when CP violating phases are large. In Sec. 4 we give some concluding remarks.

## II. MUON MAGNETIC MOMENT AND ELECTRON EDM

We consider here supergravity models which are a generalization of mSUGRA to include the possibility of phases in the soft breaking masses at the GUT scale  $M_G \cong 2 \times 10^{16}$  GeV. The magnitude of the soft breaking masses are still assumed to be universal, but phases are not necessarily universal. Thus the SUSY parameters at  $M_G$  are  $m_0$  (the scalar soft breaking mass),  $m_{1/2i} = |m_{1/2}| \exp(i\phi_i)$   $i = 1,2,3$  (the gaugino masses for the  $U(1)$ ,  $SU(2)$ ,  $SU(3)$  groups),  $A_0 = |A_0| \exp(i\alpha_0)$  (cubic soft breaking mass),  $B_0 = |B_0| \exp(i\theta_{B_0})$  (quadratic soft breaking mass), and  $\mu_0 = |\mu_0| \exp(i\theta_\mu)$  (the Higgs mixing parameter in the superpotential).

The model therefore depends on five magnitudes and six phases. However, one can always set one of the gaugino phases to zero, and we chose here  $\phi_2 = 0$ .

The renormalization group equations (RGEs) allow one to evaluate the parameters at the electroweak scale. To one loop order, the  $\phi_i$  and  $\theta_\mu$  do not run. Further, radiative breaking of  $SU(2) \times U(1)$  at the electroweak scale allows one to eliminate  $\theta_\mu$  in terms of  $\theta_B$ , the  $B$  phase at the electroweak scale, and determine  $|\mu|$  and  $|B|$  in terms of the other parameters and  $\tan\beta = |\langle H_2 \rangle / \langle H_1 \rangle|$ . Thus with a convenient choice of Higgs VEV phases, the minimization of the Higgs potential yields [19]:

$$\theta_\mu = -\theta_B + f(-\theta_B + \alpha_q, -\theta_B + \alpha_l) \quad (1)$$

$$|\mu|^2 = \frac{m_1^2 - \tan^2\beta m_2^2}{\tan^2\beta - 1}; \quad |B| = \frac{1}{2} \sin 2\beta \frac{m_3^2}{|\mu|} \quad (2)$$

where  $\alpha_q$  and  $\alpha_l$  are the quark and lepton phase of  $A_q$  and  $A_l$  at the electroweak scale,  $m_i^2 = m_{H_i}^2 + \Sigma_i$  ( $i = 1, 2$ ),  $m_3^2 = 2|\mu|^2 + m_1^2 + m_2^2$ , and  $m_{H_i}$  are the Higgs running masses at the electroweak scale.  $\Sigma_i = dV_1/dv_i^2$  where  $V_1$  is the one loop contribution to the Higgs potential, and  $v_i = |\langle H_i \rangle|$ . There remain therefore four real parameters which we take to be  $m_0$ ,  $|A_0|$ ,  $|m_{1/2}|$  and  $\tan\beta$ , and four phases  $\theta_{B_0}$ ,  $\alpha_0$ ,  $\phi_1$  and  $\phi_3$ . In this paper we examine only the electron electric dipole moment<sup>2</sup> (eEDM), and so our results are only very weakly dependent on  $\phi_3$ . Also, since we are dealing only with first and second generation sleptons, there is only a weak dependence on  $\alpha_0$ . Thus the two important phases are  $\theta_{B_0}$  and  $\phi_1$ . The parameter range that we examine is:

$$|m_0| < 1 \text{ TeV}; \quad |m_{1/2}| < 1 \text{ TeV}; \quad |A_0/m_{1/2}| < 4 \quad (3)$$

$$\tan\beta \leq 40 \quad (4)$$

As discussed above, both  $a_\mu$  and  $d_e$  can be obtained from the same complex amplitude  $A$  (assuming universal soft breaking in the first two generations). One has then

$$a_\mu = -\frac{\alpha}{4\pi \sin^2\theta_W} m_\mu^2 \text{Re}[A] \quad (5)$$

$$d_e/e = -\frac{\alpha}{8\pi \sin^2\theta_W} m_e \text{Im}[A] \quad (6)$$

The amplitude  $A$  is defined in the Appendix. For the case where there are no CP violating phases, the experimental  $a_\mu$  data [7] favors large  $\tan\beta$  [8]. In order to see semi-quantitatively the nature of the cancellations needed to make  $d_e$  small, the leading terms for large  $\tan\beta$  were obtained in the Appendix when  $\mu^2 \gg M_W^2$  (which is almost always the case for the

---

<sup>2</sup>While there has been considerable progress in calculating the neutron EDM [20] and <sup>199</sup>Hg EDM [5], there remain still significant hadronic uncertainties, in contrast to the clear calculation of the eEDM. Further, the  $\phi_3$  phase can always be adjusted to satisfy the neutron EDM, and the effect of the <sup>199</sup>Hg EDM would then only result in reducing the remaining parameter space that we find from the eEDM and the muon  $g - 2$  given here.

mSUGRA parameter space). From Eqs. (A18, A25) we find for the neutralino and chargino diagrams

$$a_\mu = a(\tilde{\chi}^\pm) + a(\tilde{\chi}^0) \quad (7)$$

where

$$a(\tilde{\chi}^\pm) = C_\mu(\tilde{\chi}^\pm) \left[ \frac{|\mu|^2}{|\mu|^2 - \tilde{m}_2^2} F_1 - \frac{\tilde{m}_2^2}{|\mu|^2 - \tilde{m}_2^2} F_2 \right] \cos \theta_\mu \quad (8)$$

$$a(\tilde{\chi}^0) = C_\mu(\tilde{\chi}^0) \left[ \left\{ \left( \frac{|\mu|^2}{m_{\tilde{u}_L}^2 - m_{\tilde{u}_R}^2} - \frac{|\mu|^2}{|\mu|^2 - \tilde{m}_1^2} \right) G_{11} \right. \right. \\ \left. \left. - \left( \frac{|\mu|^2}{m_{\tilde{u}_L}^2 - m_{\tilde{u}_R}^2} - \frac{1}{2} \frac{|\mu|^2}{|\mu|^2 - \tilde{m}_1^2} \right) G_{21} \right\} \cos(\theta_\mu + \phi_1) \right. \\ \left. - \frac{1}{2 \tan^2 \theta_W} \frac{|\tilde{m}_1|}{\tilde{m}_2} \frac{|\mu|^2}{|\mu|^2 - \tilde{m}_2^2} \left\{ \left( G_{22} - \frac{1}{2} \left( \frac{\tilde{m}_2}{|\mu|} \right)^2 G_{23} \right) \cos \theta_\mu - \frac{1}{2} \frac{\tilde{m}_2}{|\mu|} G_{23} \right\} \right] \quad (9)$$

where

$$C_\mu(\tilde{\chi}^\pm) = \frac{\alpha m_\mu^2 \tan \beta}{4\pi \tilde{m}_2 |\mu| \sin^2 \theta_W} \quad (10)$$

and  $C_\mu(\tilde{\chi}^0) = \tan^2 \theta_W (\tilde{m}_2/|\tilde{m}_1|) C_\mu(\tilde{\chi}^\pm)$ . The form factors  $F_i = F(m_{\tilde{\nu}}^2/m_{\tilde{\chi}_i^\pm}^2)$  and  $G_{ki} = G(m_{\tilde{\mu}_k}^2/m_{\tilde{\chi}_i^0}^2)$  are defined in Eqs. (A8, A12), and  $|\tilde{m}_1| \cong 0.4m_{1/2}$ ,  $\tilde{m}_2 \cong 0.8m_{1/2}$ . (Our states are labeled such that e.g.  $m_{\tilde{\chi}_i^0} < m_{\tilde{\chi}_j^0}$  for  $i < j$ .)

A similar decomposition of the electron electric dipole moment,  $d_e/e = d(\tilde{\chi}^\pm) + d(\tilde{\chi}^0)$ , gives:

$$d(\tilde{\chi}^\pm) = -D_e(\tilde{\chi}^\pm) \left[ \frac{|\mu|^2}{|\mu|^2 - \tilde{m}_2^2} F_1 - \frac{\tilde{m}_2^2}{|\mu|^2 - \tilde{m}_2^2} F_2 \right] \sin \theta_\mu \quad (11)$$

$$d(\tilde{\chi}^0) = -D_e(\tilde{\chi}^0) \left[ \left\{ \left( \frac{|\mu|^2}{m_{\tilde{u}_L}^2 - m_{\tilde{u}_R}^2} - \frac{|\mu|^2}{|\mu|^2 - \tilde{m}_1^2} \right) G_{11} \right. \right. \\ \left. \left. - \left( \frac{|\mu|^2}{m_{\tilde{u}_L}^2 - m_{\tilde{u}_R}^2} - \frac{1}{2} \frac{|\mu|^2}{|\mu|^2 - \tilde{m}_1^2} \right) G_{21} \right\} \sin(\theta_\mu + \phi_1) \right. \\ \left. - \frac{1}{2 \tan^2 \theta_W} \frac{|\tilde{m}_1|}{\tilde{m}_2} \frac{|\mu|^2}{|\mu|^2 - \tilde{m}_2^2} \left( G_{22} - \frac{1}{2} \left( \frac{\tilde{m}_2}{|\mu|} \right)^2 G_{23} \right) \sin \theta_\mu \right] \quad (12)$$

where  $D_e = (m_e/2m_\mu^2)C_\mu$ .

In the case where all phases are zero, it is well known that the chargino contribution to  $a_\mu$  dominates over the neutralino diagram even though the front factors  $C_\mu(\tilde{\chi}^\pm)$  and  $C_\mu(\tilde{\chi}^0)$  are of comparable size. This can be understood from Eqs. (8) and (9) in the following way. The second term in Eq. (8), coming from the heavy chargino,  $\tilde{\chi}_2^\pm$ , cancels about 30% of the light chargino contribution. In a similar fashion, the second term in Eq. (10) coming from

the heavy smuon,  $\tilde{\mu}_2$ , contribution cancels part of the leading term. However, due to the slowly varying nature of the form factors  $G_{11}$  and  $G_{21}$ , about 75% of the leading  $G_{11}$  term is canceled, reducing  $a(\tilde{\chi}^0)$  significantly. The remaining two terms arising from the heavy neutralinos,  $\tilde{\chi}_{2,3,4}^0$  are generally small (and there can be cancellations also between these terms). In contrast, when the CP violating phases are not zero and an electric dipole moment exists, the neutralino and chargino contributions must be of nearly equal size and opposite sign so that  $d_e$  be greatly suppressed to be in accord with experiment. This change in the relative sizes of the two terms must be brought about by the sine factors in Eqs. (11, 12). Simultaneously, the corresponding cosine factors in Eqs. (8, 9) will modify the predictions of  $a_\mu$ . This then leads to two questions:

(1) Can the experimental constraints on  $d_e$  and  $a_\mu$  (and of course all other experimental constraints) be simultaneously satisfied with “large” phases, i. e. of  $O(10^{-1})$ ?

(2) If large phases are possible (and  $d_e$  is very small) can the experimental constraints be satisfied without undue fine tuning of the phases?

Question (2) divides into two parts: (2a) Is there undue fine tuning of phases needed to satisfy the experimental constraints at the electroweak scale, and (2b) Is there undue fine tuning of the phases needed at the GUT scale? In the following, we define the fine tuning parameter  $R(\phi)$  for any phase  $\phi$  by

$$R(\phi) \equiv \frac{\phi_2 - \phi_1}{\frac{1}{2}(\phi_2 + \phi_1)} \equiv \frac{\Delta\phi}{\phi_{av}} \quad (13)$$

where  $\phi_2$  and  $\phi_1$  are the upper and lower value of  $\phi$  when the experimental constraints on  $d_e$  and  $a_\mu$  are both satisfied. We use here the current bound on  $d_e$  [21]:

$$|d_e| < 4.3 \times 10^{-27} \text{ e cm} \quad (14)$$

and the 2 std range for  $a_\mu$  [7]:

$$11 \times 10^{-10} < a_\mu < 75 \times 10^{-10} \quad (15)$$

In the following we will assume that no fine tuning less than 1% be allowed, i. e.

$$R(\phi) > 0.01 \quad (16)$$

Within this framework, we find that Question (1) can be answered affirmatively, i. e. cancellations between the neutralino and chargino diagrams in  $d_e$  can indeed be satisfied with large phases. Further, the answer to Question 2(a) is that no undue fine tuning of the electroweak parameters is necessary to achieve the suppression of  $d_e$ . However, we will see that this is not the case at the GUT scale, where the simultaneous requirements of electroweak radiative breaking and the experimental  $d_e$  constraint leads to significant fine tuning, and if Eq. (16) were imposed, a large amount of the parameter space is eliminated.

In a GUT theory, the fundamental parameters are specified at  $M_{\text{GUT}}$ , and the consequences at the electroweak scale are obtained from the renormalization group equations (RGEs). These GUT parameters are presumably to be determined at some future time by a more fundamental theory (e. g. string theory), and so fine tuning at the GUT scale may imply a significant theoretical problem (while fine tuning at the electroweak scale would be

an acceptable theoretical consequence of the RGEs). Of course, what level of fine tuning is acceptable is somewhat a matter of choice, and we view Eq. (16) only as a reasonable benchmark to consider.

In Sec. 3 below, we will consider these results in detail quantitatively. We give here an analytic discussion of how they arise. To show that large phases are easily achievable, we write  $d_e$  in the form

$$d_e/e = -D_e(\tilde{\chi}^\pm)A[\sin(\theta_\mu) + a \sin(\theta_\mu + \phi_1)] \quad (17)$$

where the coefficients  $A$  and  $a$  can be read off from Eqs. (11, 12). In the extreme case where  $d_e = 0$ , Eq. (17) and Eq. (1) imply

$$\tan \theta_B = \frac{a \sin \phi_1}{1 + a \cos \phi_1} \quad (18)$$

where we have neglected the small 1-loop correction in Eq. (1). The fact that the chargino diagram dominates over the neutralino diagram implies that  $a < 1$ , and detailed numerical calculations show that  $a \sim 0.2 - 0.4$  for much of the SUSY parameter space. Thus as  $\phi_1$  varies from 0 to  $2\pi$ , over most of the parameter space  $|\theta_B|$  will be large (rising to a maximum of about 0.5) even though  $d_e$  has been set to zero!

We next consider the effects of the CP violating phases on  $a_\mu$ . From Eqs. (8, 9), we have

$$a_\mu = C_\mu(\tilde{\chi}^\pm)A[\cos(\theta_\mu) + a \cos(\theta_\mu + \phi_1) + b] \quad (19)$$

where  $b$  is the term in Eq. (9) independent of the phases. In general,  $b$  is quite small, and we will neglect it in the following. (Of course, in the numerical calculations in Sec. 3 all such effects as well as the loop corrections are considered.) Using Eq. (18) to eliminate  $\theta_B$ , we obtain

$$a_\mu = \pm a_\mu(0) Q(a, \phi_1) \quad (20)$$

where  $a_\mu(0)$  is the value of  $a_\mu$  with zero phases,

$$Q = \frac{[1 + 2a \cos \phi_1 + a^2]^{1/2}}{(1 + a)} \leq 1 \quad (21)$$

The  $\pm$  factor in Eq. (20) is the sign of  $\cos \theta_B$ . Since experimentally,  $a_\mu > 0$ , this implies

$$\theta_B > 0 \quad \text{for } 0 < \phi_1 < \pi; \quad \theta_B < 0 \quad \text{for } \pi < \phi_1 < 2\pi \quad (22)$$

The two branches of Eq. (22) are symmetric, and in the following we consider the  $\theta_B > 0$  branch. The factor  $Q$  in Eq. (21) reduces the theoretically expected size for  $a_\mu$ . Since the experimental lower bound on  $a_\mu$  implies an upper bound on  $m_{1/2}$  [8], the  $Q$  factor due to the phases will reduce this upper bound, further restricting the allowed SUSY parameter space. However, since in general  $Q \gtrsim 0.5$ , this reduction will still be consistent with all experimental data, and the effect of the SUSY CP violating phases does not qualitatively change the fit to the data for  $a_\mu$  that was obtained assuming no CP violating phases.

We can also estimate how much fine tuning is needed in the phases to satisfy the experimental bound of Eq. (14). Thus let  $\Delta\theta_B$  be the change in  $\theta_B$  for a fixed value of  $\phi_1$  as  $d_e/e$

varies from  $-4.3 \times 10^{-27}$  cm to  $+4.3 \times 10^{-27}$  cm. Characteristically, the factor  $D(\tilde{\chi}^\pm)A$  in Eq. (17) is numerically about 100 times the current upper bound on  $d_e$  (e.g. for  $m_{1/2} = 480$  GeV ( $m_0 = 118$  GeV),  $|\mu| = 690$  GeV and  $\tan\beta = 15$ , this factor is  $4.1 \times 10^{-25}$  cm.) Considering then the variation of  $\theta_B$  in Eq. (17) one finds

$$2 \times 10^{-2} \cong \Delta\theta_B \cos(\theta_B)[1 + a \cos(\phi_1) + a \sin(\phi_1) \tan(\theta_B)] \quad (23)$$

Hence using Eq. (18),

$$R(\theta_B) \cong \Delta\theta_B / \sin(\theta_B) \cong 2 \times 10^{-2} / (a \sin(\phi_1)) \quad (24)$$

Thus the allowed range of  $\theta_B$  is indeed small, though the condition of Eq. (16) is generally satisfied. A reduction of  $d_e$  by a factor of 10 would be enough to produce a serious fine tuning problem at the electroweak scale. In contrast, we will see below that there is already a significant fine tuning problem at the GUT scale even with the current bound on  $d_e$ .

### III. DETAILED CALCULATIONS

In this section, we consider detailed calculations of the effects of the experimental constraints involving the eEDM and  $a_\mu$  which were analytically estimated in Sec. 2. The analysis is done within the framework of the generalized mSUGRA described in Sec. 2 (though extension to non-universal soft breaking models can easily be done). In order to get a clear picture of what constraints on the SUSY parameter space arise, it is necessary to simultaneously impose all the experimental constraints. Aside from the above, these include the following: (1) The LEP Higgs mass lower bound  $m_h > 114$  GeV [22]. Since the theoretical analysis of  $m_h$  still has about a 3 GeV uncertainty, (which (conservatively) may be an overestimate) we interpret this in the theoretical calculation [15] to mean  $m_h > 111$  GeV. (2) The  $b \rightarrow s\gamma$  branching ratio constraint. We take here a 2 std range of the experimental CLEO data [23]

$$1.8 \times 10^{-4} \leq BR(B \rightarrow X_s\gamma) \leq 4.5 \times 10^{-4} \quad (25)$$

In the theoretical analysis we include the NLO SUSY contribution for large  $\tan\beta$  [24], as these produce significant effects (particularly since the  $a_\mu$  lower bound favors larger values of  $\tan\beta$ ). (4) We include the 1-loop corrections to the  $b$  and  $\tau$  masses [25], which are significant also for large  $\tan\beta$ . (5) All co-annihilation effects are included in the relic density calculations. We assume here the range for the neutralino cold dark matter to be

$$0.025 < \Omega_{\tilde{\chi}_1^0} h^2 < 0.25 \quad (26)$$

The upper bound is consistent with recent Boomerang and Maxima measurements [26,27], while the lower bound allows for the possibility that there may be more than one type of dark matter. However, our calculations here are insensitive to the precise value of the lower bound, and one would get very similar results if the lower bound were raised to 0.05 or 0.1.

The effects of the Higgs mass and  $b \rightarrow s\gamma$  bounds is to push the allowed parameter space mostly into the co-annihilation domain of the relic density calculation. (Thus only a small part of the allowed parameter space occurs at small enough  $m_{1/2}$  to lie below the region of co-annihilation, which begins at  $m_{1/2} \cong 350 - 400$  GeV.) In SUGRA models, stau -



neutralino co-annihilation can occur quite naturally. Thus for  $m_0 = 0$ , the charged sleptons lie below the lightest neutralino,  $\tilde{\chi}_1^0$ , and one must increase  $m_0$  to raise their masses so that the  $\tilde{\chi}_1^0$  is the dark matter particle. Thus as  $m_{1/2}$  increases,  $m_0$  must be increased in lock step so that the neutralino remains the LSP, and one finds a relatively narrow corridor in the  $m_0 - m_{1/2}$  plane consistent with the relic density bound of Eq. (26) and with the lightest stau lying above the neutralino. The dependence of these corridors on  $\tan\beta$  and  $A_0$  are shown in Figs. 1 and 2 for the case where there are no SUSY CP violating phases. We see that the corridors (which are characteristically 20-30 GeV wide) lie higher for larger  $\tan\beta$  and larger  $|A_0|$ . This is because the stau mass decreases when these parameters are increased, and so one must raise  $m_0$  to keep the stau mass greater than the neutralino<sup>3</sup>. In general, the effect of co-annihilation is to determine  $m_0$  approximately in terms of  $m_{1/2}$  for a given  $\tan\beta$  and  $A_0$ . This greatly sharpens the predictions of the theory.

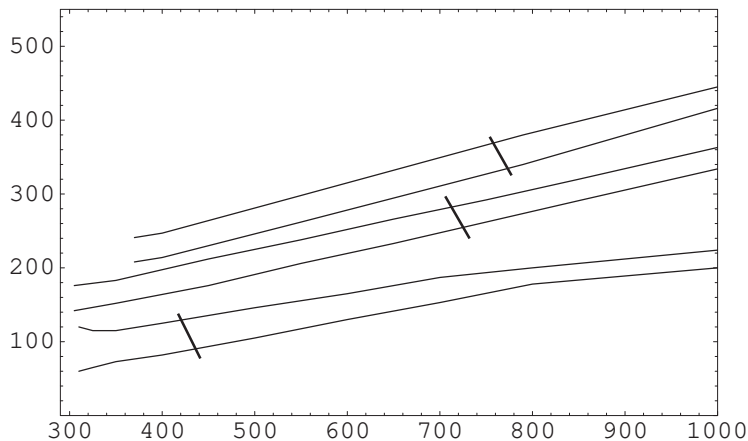


FIG. 1. Corridors in the  $m_0 - m_{1/2}$  plane allowed by the relic density constraint for (bottom to top)  $\tan\beta = 10, 30, 40$  for  $m_h > 114$  GeV,  $A_0 = 0$ ,  $\mu > 0$ , all phases set to zero. The  $\tan\beta = 30$  and  $40$  corridors all lie in the co-annihilation region, while only the beginning of the  $\tan\beta = 10$  corridor is in the non co-annihilation region. The Higgs mass bound determines the lower  $m_{1/2}$  bound for  $\tan\beta = 10$ , while both the Higgs mass and the  $b \rightarrow s\gamma$  bounds equally produce the lower bound for  $\tan\beta = 30$  and  $b \rightarrow s\gamma$  determines the lower bound for  $\tan\beta = 40$ . The short slanted lines represent the upper bound on  $m_{1/2}$  due to the  $a_\mu$  lower bound, of Eq. (15).

### A. Allowed Regions at the Electroweak Scale for $\theta_B$ and $\phi_1$

We now examine the effects of having non-zero CP violating phases present, and discuss the dependence of the allowed phases on the SUSY parameters. To illustrate the phenomena, we consider one low  $\tan\beta$  and one high  $\tan\beta$ . Since for no CP violating phases, one had (at

---

<sup>3</sup>Increasing  $\tan\beta$  or making  $A_0$  negative increases the magnitude of the L-R term in the stau mass matrix of Eq. (A3) and hence decreases the light stau mass. For  $A_0 > 0$ , the opposite effect occurs, but also the diagonal matrix elements of the mass matrix are reduced, and again the stau mass decreases.

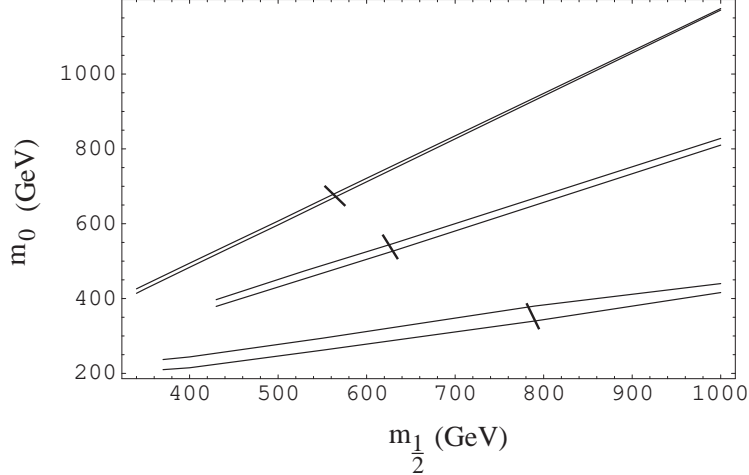


FIG. 2. Corridors in the  $m_0 - m_{1/2}$  plane allowed by the relic density constraint for (from bottom to top)  $A_0 = 0$ ,  $-2m_{1/2}$ ,  $4m_{1/2}$ , for  $m_h > 114$  GeV,  $\mu > 0$ , all phases set to zero. The lower  $m_{1/2}$  bounds for  $A_0 = 0$ ,  $-2m_{1/2}$  are due to the  $b \rightarrow s\gamma$  constraint, and for  $A_0 = 4m_{1/2}$  from the Higgs mass bound [15].

90% C.L.)  $\tan \beta > 10$ , we examine the cases of  $\tan \beta = 15$  and  $\tan \beta = 40$ . Fig. 3 shows the corridors allowed for  $\theta_B$  (the  $B$  phase at the electroweak scale) by the current experimental bounds on  $d_e$  for  $\tan \beta = 40$ ,  $A_0 = 0$  for two choices of the gaugino phase:  $\phi_1 = 0.9$  (lower curves) and  $\phi_1 = 1.2$  (upper curves). One sees that one gets a significant phase  $\theta_B$  of the size expected by Eq. (18), the larger  $\phi_1$  allowing a larger  $\theta_B$ , also in accord with Eq. (18). Note also that the allowed corridors for  $\theta_B$  widens as  $m_{1/2}$  increases as expected, since the experimental  $d_e$  constraint is less severe for a heavier mass spectrum. A similar graph is shown in Fig. 4 for  $\phi_1 = 0.9$  (upper curves),  $\phi_1 = 3.4$  (lower curves).  $\theta_B$  turns negative for  $\phi_1$  in the third quadrant, again as expected from Eq. (22).

We note in all these curves, the upper bound on  $m_{1/2}$  (due to the lower bound on  $a_\mu$ ) is reduced compared to the case when the CP violating phases are zero. (Then the upper bound is  $m_{1/2} = 790$  GeV for  $\tan \beta = 40$ ,  $A_0 = 0$  [8].) This is due to the phase  $\phi_1$  in the  $Q$  factor in Eq. (20).  $Q$  is smallest when  $\phi_1$  is near  $\pi$ , as can be seen in explicitly in Fig. 4 for  $\phi_1 = 3.4$

We consider next the  $\tan \beta$  dependence of the allowed region for  $\theta_B$ . This arises due to an indirect  $\tan \beta$  dependence in the parameter  $a$  of Eqs. (17,18). As seen from Fig. 2, coannihilation determines  $m_0$  in terms of  $m_{1/2}$ , and this  $m_0$  increases with  $\tan \beta$ , changing the ratio of neutralino to chargino diagram differentially. Fig. 5 shows the allowed region for  $\tan \beta = 15$ , and  $A_0 = 0$ ,  $\phi_1 = 1.2$  (upper curves) and  $\phi_1 = 0.9$  (lower curves). We see that one can get considerably larger values of  $\theta_B$  at lower  $\tan \beta$ , though the upper bound on  $m_{1/2}$  due to the lower bound on  $a_\mu$  is considerably reduced at low  $\tan \beta$ . The  $A_0$  dependence is exhibited in Fig. 6, where the allowed corridor for  $\theta_B$  is plotted for  $\tan \beta = 40$ ,  $\phi_1 = 0.9$  and  $A_0 = 0$  (upper curves),  $|A_0| = 2m_{1/2}$ ,  $\alpha_0 = 0.5$  (lower curves). Increasing the magnitude of  $A_0$  increases the value of  $m_0$  (by Fig. 2) and reduces the size of  $\theta_B$ .

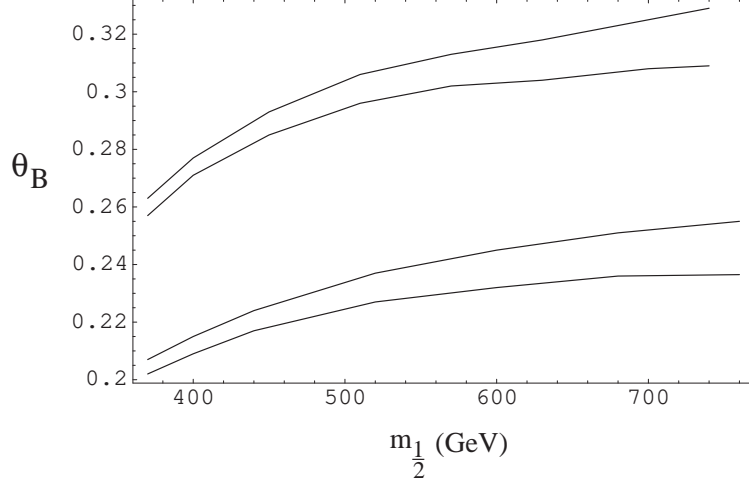


FIG. 3. Regions allowed for  $\theta_B$  by the experimental constraint on  $d_e$  as a function of  $m_{1/2}$  for  $\tan \beta = 40$ ,  $A_0 = 0$ , for  $\phi_1 = 0.9$  (lower curves) and  $\phi_1 = 1.2$  (upper curves).

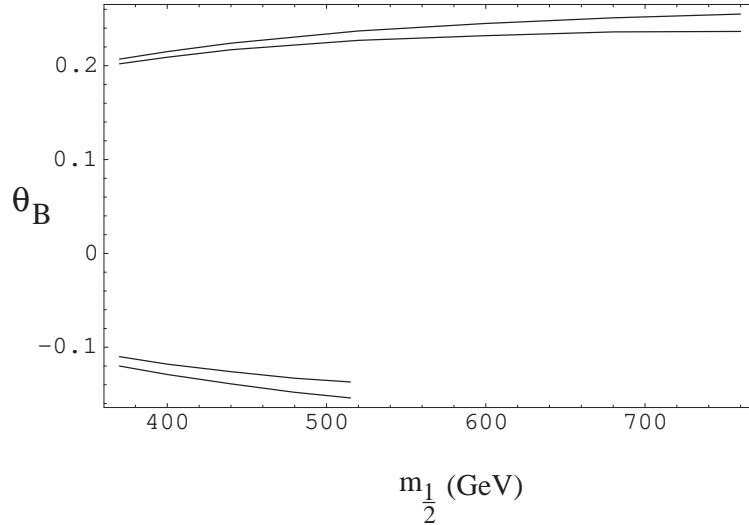


FIG. 4. Same as Fig. 3 for  $\phi_1 = 0.9$  (upper curves) and  $\phi_1 = 3.4$  (lower curves).

### B. Fine Tuning at the Electroweak Scale

The above analysis shows that the  $d_e$  experimental constraint allows  $\theta_B$  to be  $O(10^{-1})$  for a wide region of parameter space, and  $\phi_1$  can range widely, i.e. from 0 to  $2\pi$ . We next investigate whether the smallness of the upper bound on  $d_e$  requires any fine tuning to maintain this constraint. In Fig. 7 we plot the fine tuning parameter  $R$  of Eq. (13) for  $\theta_B$  for  $\tan \beta = 40$ ,  $A_0 = 0$  for  $\phi_1 = 0.9$  (upper curve) and  $\phi_1 = 1.2$  (lower curve). One sees that  $R(\theta_B)$  is small, i.e. a few percent, but satisfies the criteria  $R > 0.01$  for the entire range. The size of  $R(\theta_B)$  is consistent with what was expected from the analytic analysis of Eq. (24), and increases as  $\phi_1$  decreases also as expected. Fig. 8 shows a similar plot for  $\tan \beta = 15$ . Since  $\theta_B$  is larger here (see Fig. 5),  $R(\theta_B)$  is smaller, but still within the acceptable range. Fig. 9 shows  $R(\phi_1)$  for  $\tan \beta = 40$ ,  $A_0 = 0$  for  $\theta_B = 0.2$  (upper curve), and  $\theta_B = 0.3$  (lower curve). Again  $R(\phi_1) > 0.01$  for the entire range of  $m_{1/2}$ , and is generally larger than  $R(\theta_B)$ .

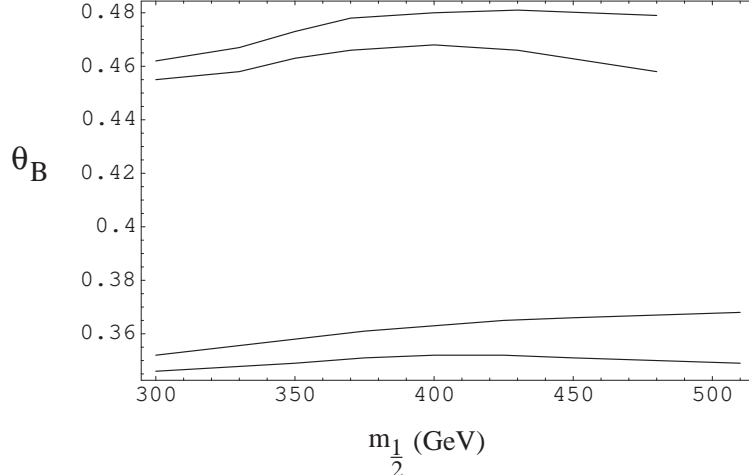


FIG. 5. Same as Fig. 3 for  $\tan\beta = 15$ . The allowed regions terminate at low  $m_{1/2}$  due to the  $m_h$  constraint.

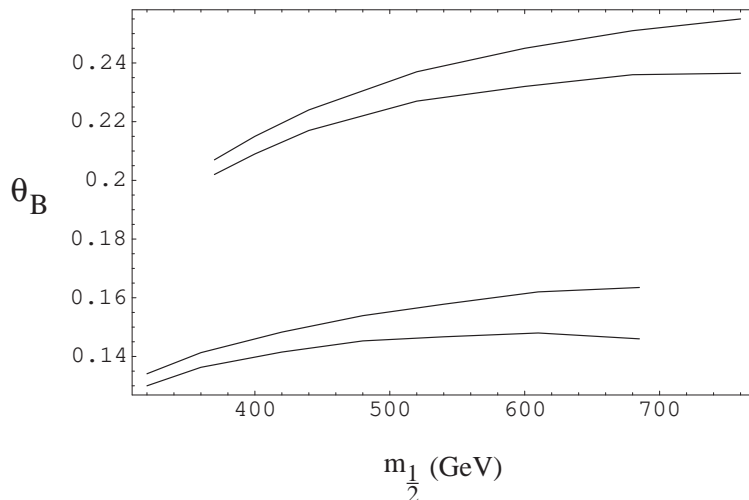


FIG. 6. Allowed region for  $\theta_B$  for  $\tan\beta = 40$  for  $A_0 = 0$  (upper curves) and  $|A_0| = 2m_{1/2}$ ,  $\alpha_0 = 0.5$  (lower curves).

(by about a factor of  $\tan\phi_1/\phi_1$ ).

We see from the above results that the current experimental bound on  $d_e$  can be accommodated with large phases. Further, for most of the parameter space, while the range of the allowed phases at the electroweak scale required to accommodate the bound on  $d_e$  is small, no fine tuning below 1% is needed. We will see, however, a more serious fine tuning problem develops at the GUT scale.

### C. Fine Tuning at the GUT Scale

We now examine what parameters are fine tuned at the GUT scale to achieve the experimental EDM bounds. From Eq. (1), we see since the loop correction is small, that  $\theta_\mu \cong -\theta_B$ , and since we have seen that  $\theta_B$  does not need excessive fine tuning, the same can be said for  $\theta_\mu$ . Further, since  $\theta_\mu$  does not run with the RGE, its value at the GUT scale is the same as

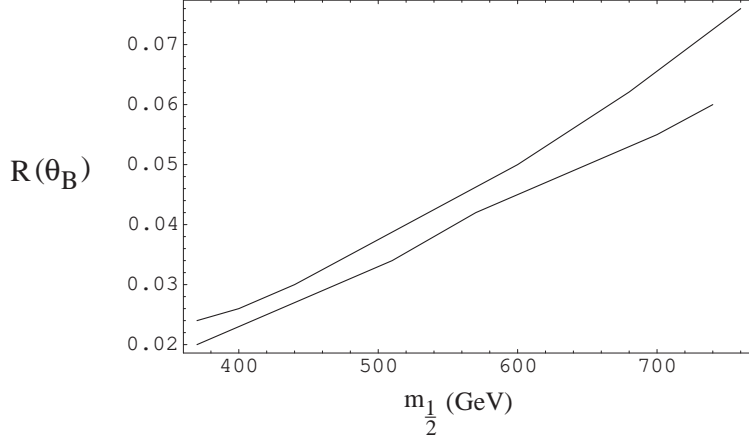


FIG. 7.  $R(\theta_B)$  as a function of  $m_{1/2}$  for  $\tan \beta = 40$ ,  $A_0 = 0$ ,  $\phi_1 = 0.9$  (upper curve),  $\phi_1 = 1.2$  (lower curve).

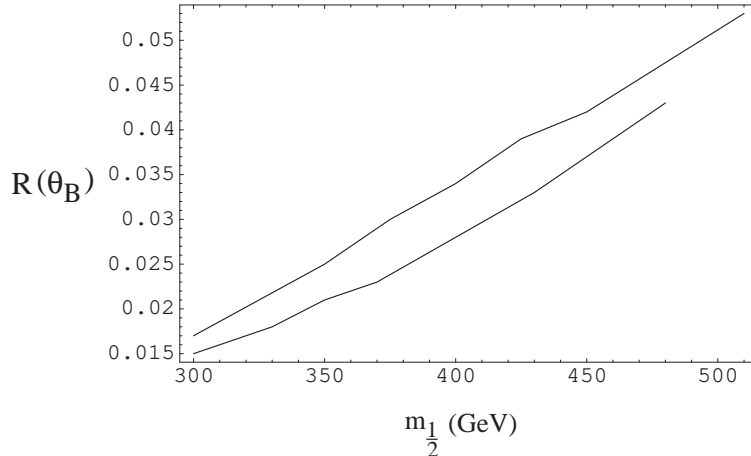


FIG. 8. Same as Fig. 7 for  $\tan \beta = 15$ .

at the electroweak scale and hence no fine tuning is needed at  $M_G$ . A similar result holds for  $\phi_1$ , which also does not run with the RGE. However, as has been previously pointed out [4], matters are different for the  $B$  phase at  $M_G$ ,  $\theta_{B_0}$ , and we review briefly the discussion given there<sup>4</sup>. To see analytically what is occurring, we consider the intermediate and low  $\tan \beta$  region, where the RGE can be analytically solved. One finds for  $B$  the result [4]

$$B = B_0 - \frac{1}{2}(1 - D_0) - \sum \Phi_i |m_{1/2}| e^{i\phi_i} \quad (27)$$

where  $D_0 = 1 - (m_t/\sin \beta)^2 \lesssim 0.25$  and  $\Phi_i = O(1)$ . As  $\tan \beta$  gets large, the radiative breaking condition Eq. (2) shows that  $|B|$  gets small. Taking the imaginary part of Eq. (27) gives

---

<sup>4</sup>This analysis differs from that given in [28] which does not take into account the possibility of cancellations in  $d_e$  between the neutralino and chargino diagrams. In fact the discussion in [28] sets the phase  $\theta_{B_0}$  to zero.

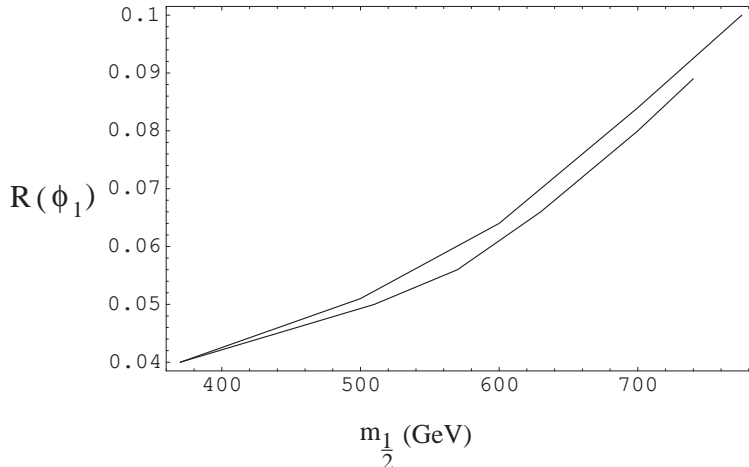


FIG. 9.  $R(\phi_1)$  as a function of  $m_{1/2}$  for  $\tan \beta = 40$ ,  $A_0 = 0$  and  $\theta_B = 0.2$  (upper curve),  $\theta_B = 0.3$  (lower curve).

$$|B| \sin \theta_B = |B_0| \sin \theta_{B_0} - (1/2)(1 - D_0)|A_0| \sin \alpha_0 - \sum \Phi_i |m_{1/2}| \sin \phi_i \quad (28)$$

To the lowest approximation, since  $|B|$  is small, one may then neglect the lhs of Eq. (28). Eq. (28) may then be viewed as an equation determining  $\theta_{B_0}$  in terms of the other GUT scale phases, and hence  $\theta_{B_0}$  will in general be large if the other phases are not all small (a result that is confirmed in [4] by detailed calculation). However, the range of  $\theta_{B_0}$  so that the experimental bound on  $d_e$  is satisfied is then significantly reduced. Thus for fixed values of  $\alpha_0$  and  $\phi_i$ , Eq. (28) gives as  $\tan \beta$  gets large (i.e.  $|B|$  becomes small)

$$\Delta \theta_{B_0} \cong (|B|/|B_0|)\Delta \theta_B \ll \Delta \theta_B \quad (29)$$

Since we have already seen that  $\Delta \theta_B$  is small (though not violating the fine tuning condition), one may expect that  $\Delta \theta_{B_0}$  may need to be fine tuned, particularly for low  $m_{1/2}$  where the SUSY mass spectrum is light. This is seen explicitly in Fig. 10 for  $\tan \beta = 40$ ,  $A_0 = 0$  with  $\phi_1 = 0.9, 1.2, 1.6, 2.3$ , and  $2.6$ . We see that  $R(\theta_{B_0})$  decreases as  $\phi_1$  increases from  $0.9$  to  $1.6$  ( $\cong \pi/2$ ) and then increases for  $2.3$  and  $2.6$  where  $\pi - \phi_1$  is decreasing. (The upper bound on  $m_{1/2}$  arising from the lower bound on  $a_\mu$  decreases as  $\phi_1$  moves into the second quadrant in accord with Eqs. (20,21).) We see that if one imposes the fine tuning constraint that  $R(\theta_{B_0}) > 0.01$ , large sections of the low  $m_{1/2}$  region would be excluded, e. g. one would require  $m_{1/2} > 540$  GeV for  $\phi_1 = 1.6$ . The fine tuning becomes more acute at lower values of  $\tan \beta$ . Thus Fig. 11 shows  $R(\theta_{B_0})$  as a function of  $m_{1/2}$  for  $\tan \beta = 15$ ,  $A_0 = 0$  for  $\phi_1 = 0.9$  (upper curve) and  $\phi_1 = 1.2$  (lower curve). Thus the fine tuning constraint would eliminate completely  $\phi_1 = 1.2$  (and the entire region of  $\sim 0.4$  radians around  $\pi/2$ ) and also restricts the other values of  $\phi_1$ . Finally, we note that increasing  $A_0$  generally increases the amount of fine tuning needed. Thus Fig. 12 shows  $R(\theta_{B_0})$  for  $\tan \beta = 40$ ,  $\phi_1 = 0.9$  for  $A_0 = 0$  (upper curve) and  $|A_0| = 2m_{1/2}$ ,  $\alpha_0 = 0.5$  (lower curve). The entire  $|A_0| = 2m_{1/2}$  curve has  $R(\theta_{B_0}) < 0.001$ .

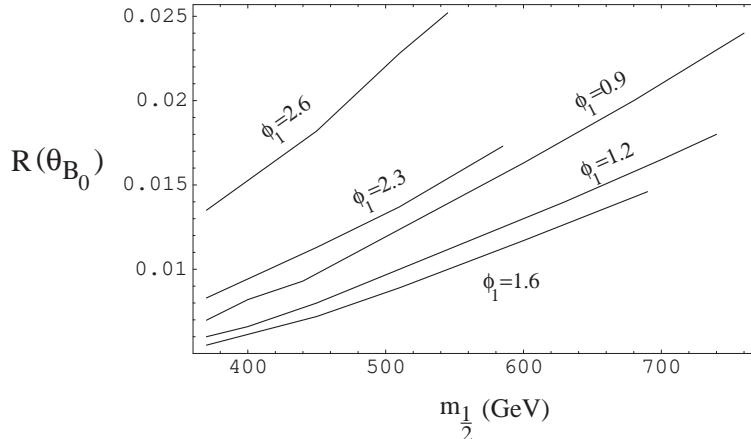


FIG. 10.  $R(\theta_{B_0})$  as a function of  $m_{1/2}$  for  $\tan\beta = 40$ ,  $A_0 = 0$  for (from bottom to top)  $\phi_1 = 1.6, 1.2, 0.9, 2.3$  and  $2.6$ .

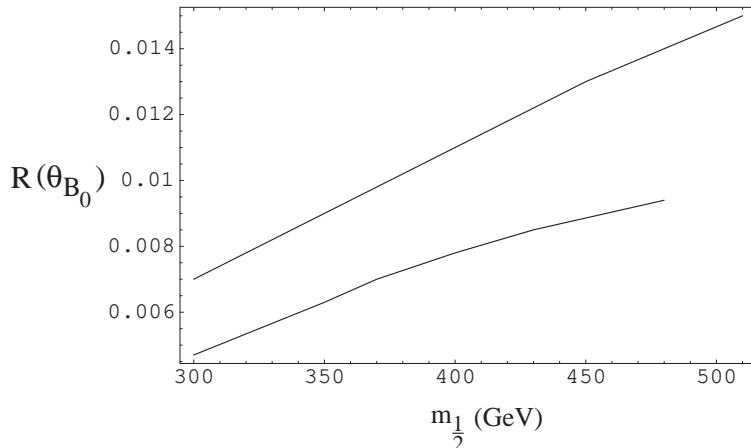


FIG. 11.  $R(\theta_{B_0})$  as a function of  $m_{1/2}$  for  $\tan\beta = 15$ ,  $A_0 = 0$  for  $\phi_1 = 0.9$  (upper curve) and  $\phi_1 = 1.2$  (lower curve)

#### IV. CONCLUSIONS

We have examined here what SUSY CP violating phases are possible within the framework of SUGRA models, when the electron electric dipole moment experimental bound is imposed on the SUSY parameter space. In order to analyze this, we imposed simultaneously the accelerator bounds of the Higgs mass ( $m_h > 114$  GeV) and the  $b \rightarrow s\gamma$  branching ratio, the relic density bound for neutralino cold dark matter and the recent 2.6 std deviation of the muon magnetic moment from the Standard Model prediction. The different experimental constraints interact with each other. Thus the Higgs mass and  $b \rightarrow s\gamma$  constraints put lower bounds on the gaugino mass ( $m_{1/2} \gtrsim (300 - 400)$  GeV) which puts the relic density analysis mostly in the region where stau-neutralino co-annihilation occurs. This closely fixes the scalar mass  $m_0$  in terms of  $m_{1/2}$  (for fixed  $A_0$  and  $\tan\beta$ ). The  $a_\mu$  lower bound then puts an upper bound on  $m_{1/2}$ . Thus the parameter space becomes highly constrained. One can estimate analytically, as was done in Sec. 2, the effects of turning on the CP violating phases. In fact if  $d_e$  were zero, one could still have large CP violating phases present, with the Bino phase  $\phi_1$  between 0 and  $2\pi$ . The condition that  $a_\mu$  be positive puts the  $B$  phase

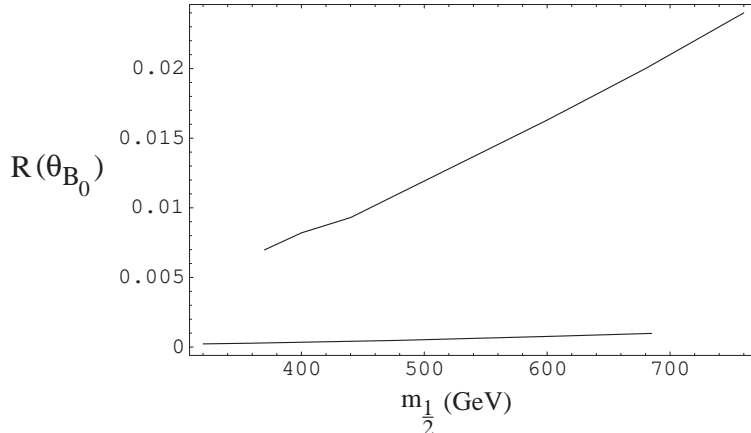


FIG. 12.  $R(\theta_{B_0})$  as a function of  $m_{1/2}$  for  $\tan \beta = 40$ ,  $\phi_1 = 0.9$  for  $A_0 = 0$  (upper curve) and  $|A_0| = 2m_{1/2}$ ,  $\alpha_0 = 0.5$  (lower curve).

$\theta_B$  in the first and fourth quadrants with  $|\theta_B| \sim 0.2 - 0.4$ . The dependence of  $\theta_B$  on  $\tan \beta$  and  $A_0$  was discussed in detail in Sec. 3. It was seen that the phase  $\phi_1$  acts to reduce the theoretical value of  $a_\mu$  by a factor  $Q < 1$ , defined in Eq. (20, 21), and from the experimental lower bound on  $a_\mu$  this reduces the upper bound on  $m_{1/2}$ , limiting further the parameter space.

The relevant question, however, is whether the smallness of the experimental bound on  $d_e$  requires an unreasonable amount of fine tuning of the phases. Using the parameter  $R(\phi) = \Delta\phi/\phi_{av}$ , we find at the electroweak scale, both  $R(\theta_B)$  and  $R(\phi_1)$  are small, i. e. a few percent. However, in general  $R > 0.01$ , and so no fine tuning below the 1% level is needed. However, at the GUT scale, this is not the case for  $R(\theta_{B_0})$  for a significant part of the parameter space. Thus if we were to exclude regions where  $R(\theta_{B_0}) < 0.01$ , then for  $\tan \beta = 15$ ,  $A_0 = 0$ ,  $\phi_1$  phases near  $90^\circ$  ( i. e.  $1.2 < \phi_1 < 2.0$ ) are completely excluded (Fig. 11). The effect is reduced for higher  $\tan \beta$ . However, for example, for  $\tan \beta = 40$ ,  $A_0 = 0$  the condition  $R > 0.01$  would eliminate  $m_{1/2} < 540$  GeV for  $\phi_1 = 1.6$ , and raise the lower bound on  $m_{1/2}$  by a lesser amount for other values of  $\phi_1$  (Fig. 10). Increasing  $A_0$  decreases the value of  $R$ , making the fine tuning more serious, as can be seen in Fig. 12.

The fine tuning problem is thus on the verge of becoming quite acute. The experimental bound on  $d_e$  is likely to decrease by a factor of three in the near future [29]. The effect this would have is shown in Figs. 13 and 14. Fig. 13 shows  $R(\theta_B)$  as a function of  $m_{1/2}$  for  $\tan \beta = 40$ ,  $A_0 = 0$ ,  $\phi_1 = 0.4$  (upper curve) (corresponding to  $\theta_B \simeq 0.1$ ) and  $\phi_1 = 0.9$  (lower curve). The curves are what would occur if the experimental bound on  $d_e$  were reduced by a factor of three. Fig. 14 shows  $R(\theta_{B_0})$  as a function of  $m_{1/2}$  for  $\tan \beta = 15$ ,  $A_0 = 0$ ,  $\phi_1 = 0.3$  (upper curve) (corresponding to  $\theta_B \simeq 0.1$ ) and  $\phi_1 = 0.9$  (lower curve), if the bound is reduced by a factor of three.  $\phi_1 < 0.4$  in Fig. 13 and  $\phi_1 < 0.3$  in Fig. 14 would have less fine tuning but correspond to  $\theta_B < 0.1$ .

In a GUT theory, presumably the parameters at the GUT scale are the more fundamental ones, and fine tuning of these parameters would presumably represent a serious problem. Of course, what level of fine tuning one accepts is somewhat a matter of taste, and we view the criteria  $R > 0.01$  as merely a bench mark for consideration. However, the above results show that any significant experimental reduction of  $d_e$  would make the idea of large



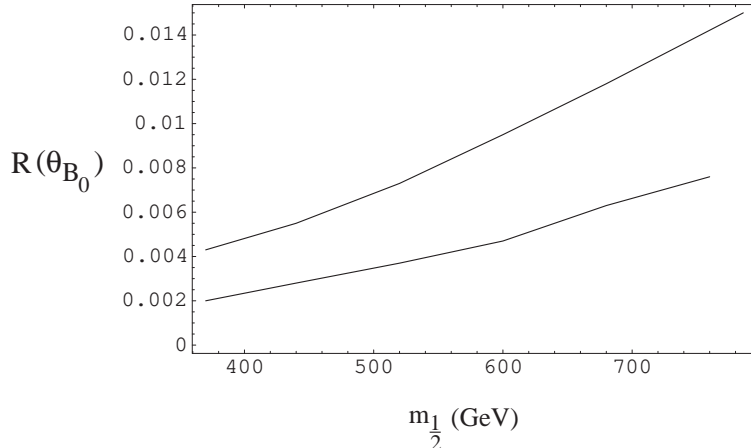


FIG. 13.  $R(\theta_B)$  as a function of  $m_{1/2}$  for  $\tan\beta = 40$ ,  $A_0 = 0$ ,  $\phi_1 = 0.9$  (lower curve) and  $\phi_1 = 0.4$  (upper curve) with the current experimental bound on  $d_e$  reduced by a factor of three.

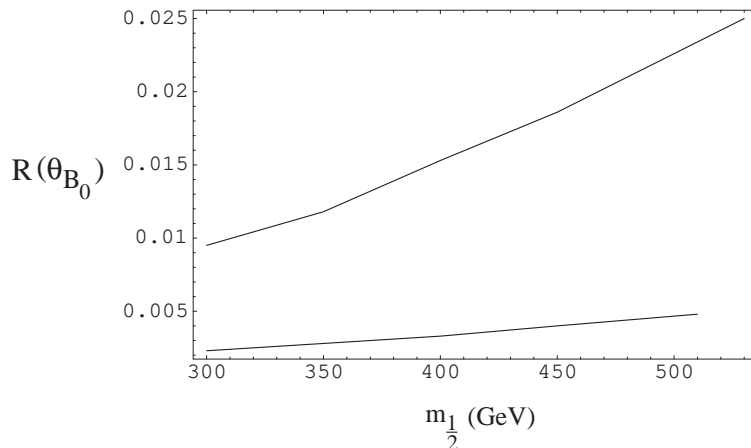


FIG. 14.  $R(\theta_{B_0})$  as a function of  $m_{1/2}$  for  $\tan\beta = 15$ ,  $A_0 = 0$ ,  $\phi_1 = 0.9$  (lower curve) and  $\phi_1 = 0.3$  (upper curve) with the current experimental bound on  $d_e$  reduced by a factor of three.

SUSY CP violating phases more difficult to maintain, as fine tuning would set in even at the electroweak scale unless the SUSY masses are heavy.

This work was supported in part by National Science Foundation grant No. PHY-0070964.

## APPENDIX A: DERIVATIONS

In this Appendix, we calculate the leading terms in  $\tan\beta$  for the complex amplitude  $A$  of Eqs. (5) and (6) needed to calculate  $a_\mu$  and  $d_e$ . In order to do this, it is necessary to diagonalize the various mass matrices entering in the chargino and neutralino loops. These matrices depend on the phases  $\phi_1$ ,  $\alpha_l$  and  $\theta = \theta_\mu + \epsilon_1 + \epsilon_2$  where  $\alpha_l$  is the phase of  $A_l$  and  $\langle H_{1,2} \rangle = v_{1,2} e^{i\epsilon_{1,2}}$  where  $v_{1,2} = |\langle H_{1,2} \rangle|$ . Minimizing the effective potential with respect to  $\epsilon_{1,2}$  determines  $\theta$  in terms of  $\theta_B$ , and one may then choose Higgs phases such that  $\epsilon_{1,2} = 0$ , as was done in Eq. (1). With this choice of phases, the chargino and neutralino mass matrices are

$$M_{\tilde{\chi}^\pm} = \begin{pmatrix} \tilde{m}_2 & \sqrt{2}M_W \sin \beta \\ \sqrt{2}M_W \cos \beta & \mu \end{pmatrix} \quad (\text{A1})$$

$$M_{\tilde{\chi}^0} = \begin{pmatrix} \tilde{m}_1 & 0 & a & b \\ 0 & \tilde{m}_2 & c & d \\ a & c & 0 & -\mu \\ b & d & -\mu & 0 \end{pmatrix} \quad (\text{A2})$$

where  $\tilde{m}_1 = |\tilde{m}_1|e^{i\phi_1}$ ,  $\mu = |\mu|e^{i\theta_\mu}$ ,  $a = -M_Z \sin \theta_W \cos \beta$ ,  $b = M_Z \sin \theta_W \sin \beta$ ,  $c = -a \cot \theta_W$ ,  $d = -b \cot \theta_W$ , and  $\tilde{m}_2$  has been chosen real and positive.

The slepton mass matrices have the form

$$M_l^2 = \begin{pmatrix} m_{lLL}^2 & m_{lLR}^2 \\ m_{lLR}^{2*} & m_{lRR}^2 \end{pmatrix} \quad (\text{A3})$$

where  $m_{lLR}^2 = m_l(A_l^* - \mu \tan \beta)$ ,  $A_l = |A_l|e^{i\alpha_l}$ , and

$$m_{lLL}^2 = m_L^2 + m_l^2 - \frac{1}{2}(1 - 2 \sin^2 \theta_W)M_Z^2 \cos 2\beta \quad (\text{A4})$$

$$m_{lRR}^2 = m_R^2 + m_l^2 - \sin^2 \theta_W M_Z^2 \cos 2\beta \quad (\text{A5})$$

The  $m_{L,R}^2$  are obtained by running the RGE from the GUT scale to the electroweak scale [30]. In our analysis we will assume universal soft breaking of the  $\tilde{\mu}$  and  $\tilde{e}$  scalar masses ( $m_0$ ) and universal cubic soft breaking masses ( $A_0$ ) at  $M_G$ . Since  $m_e^2$  and  $m_\mu^2$  are very small, they can be neglected at the electroweak scale, i.e.,  $M_\mu^2 = M_e^2$ .

$M_{\tilde{\chi}^0}$  is a symmetric, complex matrix and can be diagonalized by a unitary matrix  $X$  according to  $M_{\tilde{\chi}^0}X = X^*M_{\tilde{\chi}^0}^{(D)}$  where

$$M_{\tilde{\chi}^0}^{(D)} = \text{diag}(m_{\tilde{\chi}_1^0}, m_{\tilde{\chi}_2^0}, m_{\tilde{\chi}_3^0}, m_{\tilde{\chi}_4^0}) \quad (\text{A6})$$

$M_l^2$  can be diagonalized by a hermitian matrix  $D$  with  $M_l^2 D = D M_l^{2(D)}$  where  $M_l^{2(D)} = \text{diag}(m_{l_1}^2, m_{l_2}^2)$ . Finally one diagonalizes  $M_{\tilde{\chi}^\pm}$  by two unitary transformations  $U$  and  $V$  according to  $U^* M_{\tilde{\chi}^\pm} V^\dagger = M_{\tilde{\chi}^\pm}^{(D)}$  where  $M_{\tilde{\chi}^\pm}^{(D)} = \text{diag}(m_{\tilde{\chi}_1^\pm}, m_{\tilde{\chi}_2^\pm})$ .

The amplitude  $A$  can be divided into its chargino and neutralino parts:  $A = A(\tilde{\chi}^\pm) + A(\tilde{\chi}^0)$ . We follow the notation of [31] where one finds that

$$A(\tilde{\chi}^\pm) = \frac{1}{\sqrt{2}M_W \cos \beta} \sum_i \frac{1}{m_{\tilde{\chi}_i^\pm}} U_{i2}^* V_{i1}^* F_i \quad (\text{A7})$$

and  $F_i = F(m_{\tilde{\nu}}^2/m_{\tilde{\chi}_i^\pm}^2)$  with

$$F(x) = \frac{1 - 3x}{(1 - x)^2} - \frac{2x^2 \ln x}{(1 - x)^3} \quad (\text{A8})$$

Similarly

$$A(\tilde{\chi}^0) = \frac{1}{m_l} \sum_{k,j} \frac{1}{m_{\tilde{\chi}_j^0}} \left( \eta_j^k G_{kj} + \frac{m_l}{6} X_j^k H_{kj} \right) \quad (\text{A9})$$

where

$$\eta_j^k = - \left[ \frac{1}{\sqrt{2}} (\tan \theta_W X_{1j} + X_{2j}) D_{1k}^* - \kappa_l X_{3j} D_{2k}^* \right] \times \left[ \sqrt{2} \tan \theta_W X_{1j} D_{2k} + \kappa_l X_{3j} D_{1k} \right], \quad (\text{A10})$$

$$X_j^k = \frac{1}{2} \tan^2 \theta_W |X_{1j}|^2 \left( |D_{1k}|^2 + 4|D_{2k}|^2 \right) + \frac{1}{2} |X_{2j}|^2 |D_{1k}|^2 + \tan \theta_W |D_{1k}|^2 X_{1j} X_{2j}^* + O(m_l) \quad (\text{A11})$$

and  $\kappa_l = m_l / (\sqrt{2} M_W \cos \beta)$ . The loop integrals are  $G_{kj} = G(m_{\tilde{l}_k}^2 / m_{\tilde{\chi}_j^0}^2)$ ,  $H_{kj} = H(m_{\tilde{l}_k}^2 / m_{\tilde{\chi}_j^0}^2)$  where

$$G(x) = \frac{1+x}{(1-x)^2} + \frac{2x}{(1-x)^3} \ln x \quad (\text{A12})$$

$$H(x) = \frac{2+5x-x^2}{(1-x)^3} + \frac{6x}{(1-x)^4} \ln x \quad (\text{A13})$$

We need only keep the terms in  $A$  independent of  $m_l$  and thus can neglect the  $O(m_l)$  terms in Eq. (A11). (Actually,  $\eta_l^k$  begins linearly in  $m_l$ .)

We are interested in calculating only the leading terms in  $\tan \beta$ . We will also do this in the limit  $M_W^2 / |\mu|^2 \ll 1$  and  $M_W^2 / |\tilde{m}_i|^2 \ll 1$  (which is valid for most of the mSUGRA parameter space). In that case one has [32]

$$m_{\tilde{\chi}_1^0} \cong |\tilde{m}_1|; \quad m_{\tilde{\chi}_2^0} \cong m_{\tilde{\chi}_1^\pm} \cong \tilde{m}_2; \quad m_{\tilde{\chi}_{3,4}^0} \cong m_{\tilde{\chi}_2^\pm} \cong |\mu| \quad (\text{A14})$$

We consider first the calculation of  $A(\tilde{\chi}^\pm)$ . Since  $V$  diagonalizes  $M_{\tilde{\chi}^\pm}^\dagger M_{\tilde{\chi}^\pm}$  and  $U^*$  diagonalizes  $M_{\tilde{\chi}^\pm} M_{\tilde{\chi}^\pm}^\dagger$  one finds for the leading terms

$$U_{12}^* \cong -\frac{1}{\mu} \sqrt{2} M_W \sin \beta \frac{|\mu|^2}{|\mu|^2 - \tilde{m}_2^2} U_{11}^* \quad (\text{A15})$$

$$V_{21} \cong \frac{1}{\tilde{m}_2} \sqrt{2} M_W \sin \beta \frac{\tilde{m}_2^2}{|\mu|^2 - \tilde{m}_2^2} V_{22} \quad (\text{A16})$$

With an appropriate choices of phases one has to lowest order  $U_{11} \cong 1 \cong U_{22}$ ,  $V_{11} \cong 1$  and

$$V_{22} \cong e^{i\theta_\mu} \quad (\text{A17})$$

Hence inserting into Eq. (A7) gives

$$A(\tilde{\chi}^\pm) = -\frac{\tan \beta}{\tilde{m}_2 |\mu|} e^{-i\theta_\mu} \left[ \frac{|\mu|^2}{|\mu|^2 - \tilde{m}_2^2} F_1 - \frac{\tilde{m}_2^2}{|\mu|^2 - \tilde{m}_2^2} F_2 \right] \quad (\text{A18})$$

To calculate the leading terms of  $A(\tilde{\chi}^0)$  it is useful to first note the size of the matrix elements  $X_{ij}$ . Thus to zeroth order in  $M_Z$

$$X_{11} \cong e^{-\frac{i}{2}\phi_1}, \quad X_{22} \cong 1 \quad (\text{A19})$$

$$X_{33} \cong -X_{43} \cong \frac{1}{\sqrt{2}}e^{-\frac{i}{2}\theta_\mu}, \quad X_{34} \cong X_{44} \cong e^{\frac{\pi i}{2}}X_{33} \quad (\text{A20})$$

Also one has  $X_{12}, X_{21}$  are  $O(M_Z^2)$  (and hence negligible) while the remaining components are  $O(M_Z)$ . To lowest order, the slepton mass eigenvalues are  $m_{\tilde{l}_1}^2 \cong m_{lRR}^2, m_{\tilde{l}_2}^2 \cong m_{lLL}^2$ , and the  $D$  matrix has the form  $D_{12} \cong 1 \cong D_{21}$  and

$$D_{11} \cong -\frac{m_l(A_l^* - \mu \tan \beta)}{m_{\tilde{l}_2}^2 - m_{\tilde{l}_1}^2} \cong -D_{22}^* \quad (\text{A21})$$

To illustrate the calculation of  $A(\tilde{\chi}^0)$  we consider the leading term when  $k = 1 = j$ . From Eq. (A10), two terms contribute to  $\eta_1^1$  for large  $\tan \beta$ :

$$\begin{aligned} \eta_1^1 = & -\left(\frac{1}{\sqrt{2}}\tan\theta_W X_{11}D_{11}^*\right)\left(\sqrt{2}\tan\theta_W X_{11}D_{21}\right) \\ & + (\kappa_l X_{31}D_{21}^*)\left(\sqrt{2}\tan\theta_W X_{11}D_{21}\right) \end{aligned} \quad (\text{A22})$$

which evaluates to

$$\eta_1^1 = -\frac{m_l \tan^2 \theta_W \tan \beta}{|\mu|} \left[ \frac{|\mu|^2}{m_{\tilde{l}_2}^2 - m_{\tilde{l}_1}^2} - \frac{|\mu|^2}{|\mu|^2 - |\tilde{m}_1|^2} \right] e^{-i(\theta_\mu + \phi_1)} \quad (\text{A23})$$

where we have used

$$X_{31} \cong \frac{M_Z \sin \theta_W \sin \beta}{\mu} \frac{|\mu|^2}{|\mu|^2 - |\tilde{m}_1|^2} X_{11} \quad (\text{A24})$$

(Note that  $\eta_1^1$  is linear in  $m_l$  and hence Eq. (A9) is not singular as  $m_l \rightarrow 0$ .) In a similar fashion one can obtain all the leading terms in Eq. (A9). (The  $X_j^k$  terms of Eq. (A11) do not contribute.) The total answer is

$$\begin{aligned} A(\tilde{\chi}^0) \cong & -\frac{\tan^2 \theta_W \tan \beta}{|\tilde{m}_1||\mu|} \left[ \left\{ \left( \frac{|\mu|^2}{m_{\tilde{l}_2}^2 - m_{\tilde{l}_1}^2} - \frac{|\mu|^2}{|\mu|^2 - |\tilde{m}_1|^2} \right) G_{11} \right. \right. \\ & \left. \left. - \left( \frac{|\mu|^2}{m_{\tilde{l}_2}^2 - m_{\tilde{l}_1}^2} - \frac{1}{2} \frac{|\mu|^2}{|\mu|^2 - |\tilde{m}_1|^2} \right) G_{21} \right\} e^{-i(\theta_\mu + \phi_1)} \right. \\ & \left. - \frac{1}{2} \frac{1}{\tan^2 \theta_W} \frac{|\mu|^2}{|\mu|^2 - \tilde{m}_2^2} \left( \frac{|\tilde{m}_1|}{\tilde{m}_2} G_{22} - \frac{1}{2} \frac{|\tilde{m}_1| \tilde{m}_2}{|\mu|^2} G_{23} \right) e^{-i\theta_\mu} \right. \\ & \left. + \frac{1}{4} \frac{1}{\tan^2 \theta_W} \frac{|\tilde{m}_1|}{|\mu|} \frac{|\mu|^2}{|\mu|^2 - \tilde{m}_2^2} G_{23} \right] \end{aligned} \quad (\text{A25})$$

We note that a large amount of cancellation occurs in this regime: terms proportional to  $G_{24}$  have all canceled with part of the  $G_{23}$  terms, and the total  $G_{14}$  contribution cancels with the  $G_{13}$  terms. Note also that the  $A(\tilde{\chi}^0)$  depends separately on two phase combinations:  $\theta_\mu + \phi_1$  and  $\theta_\mu$ , though terms depending on  $\theta_\mu + \phi_1$  are generally larger.

## REFERENCES

- [1] See e.g. BaBar Collaboration, hep-ex/0105073; BELLE Collaboration, *Nucl. Phys. A* **684**, 704 (2001); for a review see T. Hurth et al., *J. Phys. G* **27**, 1277 (2001).
- [2] T. Falk and K. Olive, *Phys. Lett. B* **375**, 196 (1996); T. Ibrahim and P. Nath *Phys. Lett. B* **418**, 98 (1998); *Phys. Rev. D* **57**, 478 (1998); Erratum-ibid.**58**, 019901 (1998); Erratum-ibid.**60**, 079903 (1999); Erratum-ibid.**60**, 119901 (1999).
- [3] T. Falk and K. Olive, *Phys. Lett. B* **439**, 71 (1998); M. Brhlik, G. Good and G. Kane, *Phys. Rev. D* **59**, 115004 (1999); M. Brhlik, L. Everett, G. Kane and J. Lykken, *Phys. Rev. Lett.* **83**, 2124 (1999); *Phys. Rev. D* **62**, 035005 (2000); A. Bartl, T. Gajdosik, W. Porod, P. Stockinger and H. Stremnitzer, *Phys. Rev. D* **60**, 073003 (1999); S. Pokorski, J. Rosiek and C. A. Savoy, *Nucl. Phys. B* **570**, 81 (2000).
- [4] E. Accomando, R. Arnowitt and B. Dutta, *Phys. Rev. D* **61**, 075010 (2000).
- [5] T. Falk, K. Olive, M. Pospelov and R. Roiban, *Nucl. Phys. B* **560**, 3 (1999).
- [6] V. Barger, T. Falk, T. Han, J. Jiang, T. Li and T. Plehn, hep-ph/0101106; S. Abel, S. Khalil and O. Lebedev, hep-ph/0103320.
- [7] H.N. Brown et.al., Muon (g-2) Collaboration, *Phys. Rev. Lett.* **86**, 2227 (2001).
- [8] J. Feng and K. Matchev, *Phys. Rev. Lett.* **86**, 3480 (2001); U. Chattopadhyay and P. Nath, hep-ph/0102157; S. Komine, T. Moroi and M. Yamaguchi, *Phys. Lett. B* **506**, 93 (2001); *Phys. Lett. B* **507**, 224 (2001); T. Ibrahim, U. Chattopadhyay and P. Nath, hep-ph/0102324; J. Hisano and K. Tobe, hep-ph/0102315; J. Ellis, D.V. Nanopoulos and K. A. Olive, hep-ph/0102331; R. Arnowitt, B. Dutta, B. Hu and Y. Santoso, *Phys. Lett. B* **505**, 177 (2001); S. Martin and J. Wells, hep-ph/0103067; H. Baer, C. Balazs, J. Ferrandis and X. Tata, hep-ph/0103280; F. Richard, hep-ph/0104106; D. Carvalho, J. Ellis, M. Gomez and S. Lola, hep-ph/0103256; S. Baek, T. Goto, Y. Okada and K. Okumura, hep-ph/0104146; Y. Kim and M. Nojiri, hep-ph/0104258.
- [9] T. Ibrahim, U. Chattopadhyay and P. Nath, hep-ph/0102324.
- [10] A.H. Chamseddine, R. Arnowitt and P. Nath, *Phys. Rev. Lett.* **49**, 970 (1982); R. Barbieri, S. Ferrara and C.A. Savoy, *Phys. Lett. B* **119**, 343 (1982); L. Hall, J. Lykken and S. Weinberg, *Phys. Rev. D* **27**, 2359 (1983); P. Nath, R. Arnowitt and A.H. Chamseddine, *Nucl. Phys. B* **227**, 121 (1983).
- [11] L. Randall and R. Sundrum, *Nucl. Phys. B* **557**, 79 (1999); G. Giudice, M. Luty, H. Murayama and R. Rattazzi, *JHEP* **9812**, 027 (1998).
- [12] M. Dine and A. Nelson, *Phys. Rev. D* **48**, 1227 (1993); M. Dine, A. Nelson and Y. Shirman, *Phys. Rev. D* **51**, 1362 (1995); M. Dine, A. Nelson, Y. Nir and Y. Shirman, *Phys. Rev. D* **53**, 2658 (1996); for a review see G. Giudice and R. Rattazzi, *Phys. Rep.* **322**, 419 (1999).
- [13] J. Feng and K. Matchev in ref. [8].
- [14] T. Han and R. Hempfling, *Phys. Lett. B* **415**, 161 (1997).
- [15] R. Arnowitt, B. Dutta and Y. Santoso, hep-ph/0102181, *Nucl. Phys. B*, in press.
- [16] J. Ellis, T. Falk, G. Ganis, K. Olive and M. Srednicki; hep-ph/0102098; M. Gomez and J. Vergados, hep-ph/0012020; M. Gomez, G. Lazarides and C. Pallis, *Phys. Rev. D* **61**, 123512 (2000); *Phys. Lett. B* **487**, 313 (2000).
- [17] D.A. Kosower, L.M. Krauss and N. Sakai, *Phys. Lett. B* **133**, 305 (1983); T.C. Yuan, R. Arnowitt, A.H. Chamseddine and P. Nath, *Z. Phys. C* **26**, 407 (1984).

- [18] J.L. Lopez, D.V. Nanopoulos and X. Wang, *Phys. Rev. D* **49**, 366 (1994); U. Chattopadhyay and P. Nath, *Phys. Rev. D* **53**, 1648 (1996); T. Moroi, *Phys. Rev. D* **53**, 6565 (1996); Erratum-ibid, **56**, 4424 (1997). M. Carena, G.F. Giudice and C.E.M. Wagner, *Phys. Lett. B* **390**, 234 (1997); T. Goto, Y. Okada and Y. Shimizu, hep-ph/9908499; T. Blazek, hep-ph/9912460; G.C. Cho, K. Hagiwara and M. Hayakawa, *Phys. Lett. B* **478**, 231 (2000); T. Ibrahim and P. Nath, *Phys. Rev. D* **62**, 015004 (2000); M. Drees, Y. Kim, T. Kobayashi and M. Nojiri, *Phys. Rev. D* **63**, 115009 (2001).
- [19] D. Demir, *Phys. Rev. D* **60**, 055006 (1999).
- [20] M. Pospelov and A. Ritz, *Phys. Rev. D* **63**, 073015 (2001); M. Hecht, C. Roberts and S. Schmidt, nucl-th/0101058.
- [21] E.D. Commins et al., *Phys. Rev. A* **50**, 2960 (1994).
- [22] P. Igo-Kimenes, Talk presented at ICHEP 2000, Osaka, Japan, July 27 - August 2, 2000.
- [23] M. Alam et al., *Phys. Rev. Lett.* **74**, 2885 (1995).
- [24] G. Degrassi, P. Gambino and G. Giudice, *JHEP* **0012**, 009 (2000); M. Carena, D. Garcia, U. Nierste and C. Wagner, *Phys. Lett. B* **499**, 141 (2001).
- [25] R. Rattazi and U. Sarid, *Phys. Rev. D* **D53**, 1553 (1996); M. Carena, M. Olechowski, S. Pokorski and C. Wagner, *Nucl. Phys. B* **426**, 269 (1994).
- [26] C. Netterfield et al., astro-ph/0104460.
- [27] A.T. Lee et al., astro-ph/0104459 .
- [28] R. Garisto and J. Wells, *Phys. Rev. D* **55**, 1611 (1997).
- [29] Private communication with David DeMille.
- [30] L. Ibanez and C. Lopez, *Nucl. Phys. B* **233**, 511 (1984).
- [31] T. Ibrahim and P. Nath, *Phys. Rev. D* **62**, 015004 (2000).
- [32] R. Arnowitt and P. Nath, *Phys. Rev. Lett.* **69**, 725 (1992).